*Proceedings of the IASS Annual Symposium 2024*
*Redefining The Art Of Structural Design*
26 – 30 August 2024, Zurich, Switzerland
P. Block, D.C. Wolf, W. Kaufmann, J. Pauli

# Design approach for a post-tensioned funicular concrete beam

Hua CHAI[*,a], Maximilian E. ORORBIA[a], Yefan ZHI[a], Ryan WELCH[b], Billie FAIRCLOTH[b], Fahimeh Yavartanoo[c], Damon (Mohammad) Bolhassani[c], Masoud AKBARZADEH[a,d]

[*,a] Polyhedral Structures Laboratory, Weitzman School of Design, University of Pennsylvania, Philadelphia, USA
Pennovation Center, 3401 Grays Ferry Ave. Philadelphia, PA, 19146
[*] hchai@upenn.edu

[b]KieranTimberlake, Philadelphia, USA
[c]The City College of New York (CCNY), New York, USA
[d]General Robotic, Automation, Sensing and Perception (GRASP) Lab, School of Engineering and Applied Science, University of Pennsylvania, Philadelphia, USA

## Abstract:

This work proposes an approach to design a structural beam with minimal material by linking the geometric form-finding method, graphic statics, with post-tensioning as well as implementing periodic anticlastic surface geometries. To determine the placement of materials, the methodology extends upon the form-finding method developed in prior work by incorporating volumetric modeling of spatial concrete geometries to increase structural stiffness while also minimizing the overall required mass to achieve the desired performance. The combined compression and tension funicular load paths optimized from graphic statics inform the placement of the post-tensioning reinforcement and the required force to eliminate tensile forces for a given applied load and place the overall structure in compression, engaging the embedded spatial concrete geometries. To further minimize material usage and to integrate the complex spatial geometries, the beam is designed such that it can be concrete 3D-printed, eliminating the need for form-work, which is a significant contributor to construction waste.

**Keywords:** Form-finding, graphic statics, post-tensioning, volumetric modeling

## 1. Introduction

The built environment is a major contributor to greenhouse gas emissions, generating around 40% of global carbon emissions [1]. Concrete, as the dominant material used in the field, contributes 8% of annual global $CO_2e$ emissions [2]. In general, the overall emissions are raised in two sources. The first is operational emissions, reflecting all the energy-related usage in the daily operating process, such as heating, cooling, and lighting. The second emission type is the embodied emissions coming directly from the materials employed in building construction. This paper focuses on reducing embodied emissions, by introducing a design approach for a beam structure with minimal concrete mass and reinforcement. In particular, the goal is to minimize the structure's volume while maintaining the capacity of the required loading scenarios.

Conventional concrete structures rely heavily on steel, rebar reinforcement, embedded within the concrete, to handle tensile forces. While necessary, most of the concrete used to support the reinforcement in the tensile regions contributes little to the overall performance. Hence, this research implements post-tensioning technology to optimize the structural form by efficiently using concrete and minimizing the steel required. Post-tensioning forces can effectively counter the tensile forces induced by the loads, placing the whole beam in compression, engaging the concrete. With added concrete engagement, the intent to continue to minimize mass is sought after by embedding Periodic Anticlastic Surfaces (PAS), which can reduce the concrete material needed while providing additional geometric stiffness. This approach is demonstrated through the design of a concrete beam.

### 1.1. Related work

#### *1.1.1. Implementation of the algebraic graphic statics*

Graphic statics, a geometry-based form-finding method, has the advantage of illustrating the real-time intuitive relationship between the force and form diagrams [3]. Extensive research and studies have designed funicular structures using graphic statics and polyhedral graphic statics [4–6]. The recent development of the algebraic formulation to graphic statics adds efficient operation of the geometric degree of freedom (GDoF). The global configuration of the form diagrams can be assigned by users conveniently through the manipulation of the area and edge length [7, 8]. The design of the form diagram can be explored seamlessly while maintaining the equilibrium status.

#### *1.1.2. The materialization of minimal and anticlastic surfaces*

Minimal surface geometries, specifically Triply Periodic Minimal Surfaces (TPMS), have been researched and implemented in various fields due to their high structural and material efficiency [9]. The geometric properties of minimal surfaces allow for a more uniform distribution of loads. This is because the surface naturally forms into shapes that evenly distribute stress across the structure, leading to designs that are inherently more stable and require less support. The related research has been investigated as the infill methodology for the concrete design [10]. The modified version of geometry, PAS, also carries the same properties in terms of the structural design aspect. The curvatures create a condition where the internal stresses due to bending in one direction are counteracted by the stresses in the perpendicular direction. This balancing act allows it to withstand larger loads compared to flat or singly curved surfaces [11].

### 1.2. Problem statement and objective

The initial form-finding method, introduced in prior research [12], did not consider the material properties and the stresses developed in the cross-section. This paper extends the methodology to consider and link both the forces developed and materials used for construction to the form and force diagrams generated from graphic statics. For example, the amount of area required for compressive stresses and the post-tensioning forces needed to counter tensile forces can be associated with the graphic static's output. The force equilibrium is verified through analysis of the section to determine the effectiveness of the reciprocal relationship between the force and form diagram.

## 2. Graphic statics model for post-tensioning

This section develops a parametric model in which the post-tensioning force magnitude is made an adjustable variable through the algebraic edge constraint operation. The result of the form diagram shows the transition between compression and tension when varying the post-tensioning forces.

### 2.1. Form-finding

The fundamental principle of graphic statics is illustrated in Figure 1, which establishes a dual relationship between the force diagram ($\Gamma$) on the left and the form diagram ($\Gamma^{\dagger}$) on the right. This duality is based on the reciprocal nature of the diagrams, where elements in one diagram have a one-to-one correspondence with elements in the other.

In the force diagram, each edge ($e_i$) represents a force vector, with the magnitude and direction of the force indicated by the length and orientation of the edge, respectively. The equilibrium of forces at each node is ensured by the closed polygons formed by the force vectors meeting at that node.

Conversely, in the form diagram, each vertex ($v_i^{\dagger}$) corresponds to a face ($f_i$) in the force diagram. The edges connecting the vertices in the form diagram represent the lines of action of the forces. The geometric configuration of the form diagram is determined by the equilibrium of forces in the force diagram.

This reciprocal correspondence is denoted by $f_i$ corresponding to $v_i^\dagger$. Furthermore, the edges in the form diagram ($e_i^\dagger$) are perpendicular to their corresponding edges in the force diagram ($e_i$), as indicated by the lines connecting the two diagrams in Figure 1.

This dual relationship enables designers to explore the different possibilities between forces and geometry in structures while ensuring that the system stays in equilibrium. The color-coded notation—red for tension and blue for compression—within the form diagrams serves as an intuitive indicator of the structural forces, facilitating immediate visual analysis.

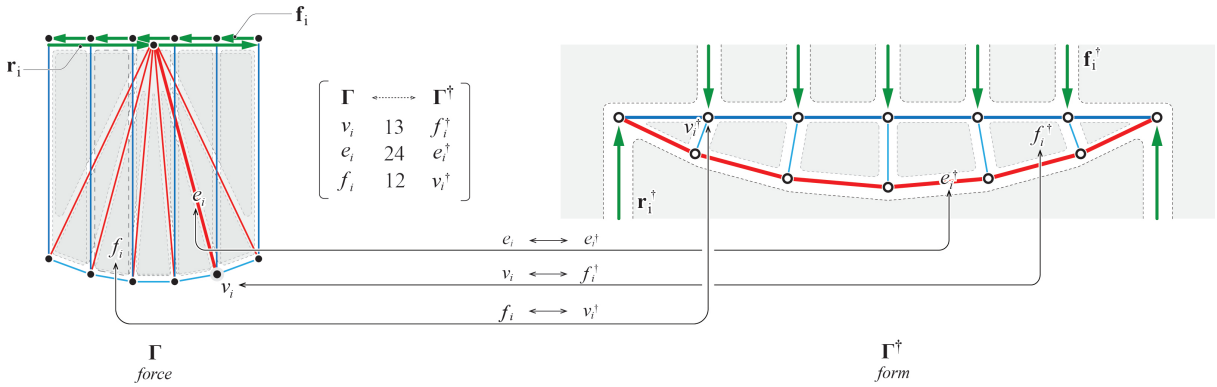


Figure 1. The reciprocal relationship between form and force diagram of the tension and compression combined structure. For 2D graphic statics, faces in the force diagram $f_i$ corresponds to vertex in form diagram $v_i^\dagger$, vertex in force $v_i$ corresponds to face in form $f_i^\dagger$, edge in force $e_i$ corresponds to edge in form $e_i^\dagger$.

The example illustrated in Figure 1 describes a spanning structure that has the reaction force acting as the support at both ends; no additional forces are added to the system. Figure 2 exemplifies a further developed application of graphic statics in the iterative process of form-finding. Each subfigure (a-d) within Figure 2 corresponds to incremental stages in the application of adjusting the edge length that represents, in this work, the post-tensioning forces and their impact on the structure's geometry.

Initially Figure 2(a) presents a starting condition devoid of any post-tensioning force ($\mathbf{f}_{\mathrm{pt_i}} = 0$), illustrated by a force diagram characterized by uniform geometry and a corresponding form diagram. The blue elements in the form diagram depict a state of pure compression across the structural members. This represents the undeformed initial geometry against which subsequent alterations are measured. Conversely, the red elements in the form diagram depict that they are in tension.

The introduction of a post-tensioning force ($\mathbf{f}_{\mathrm{pt_i}}^\dagger$), as seen in Figure 2(b), alters the force diagram, which translates algebraically to a change in the structural form. The form diagram shows that the bottom members are still in tension($\mathbf{f}_{\mathrm{btm}}^\dagger$), signified again by the red elements, a direct response to the applied post-tensioning force as visualized in the force diagram through modified edge lengths $l_{pt}$.

Figure 2(c) demonstrates the effect of increasing the post-tensioning force. Here, the structural response eliminates tension in the bottom members ($\mathbf{f}_{\mathrm{btm}}^\dagger = 0$), resulting in an adaptive geometric form to reflect the new equilibrium state. The absence of both red and blue in the bottom members of the form diagram indicates a neutral state, signifying a critical shift in the force distribution where no forces are developed in those members.

The sequence culminates in Figure 2(d) by further increasing the post-tensioning force, compelling the structure to adopt a configuration where the bottom members are now in compression, illustrated by blue curvilinear elements. This adaptation signifies a state where the force diagram, through deliberate manipulation of its edge lengths, achieves a transformed geometry with increased post-tensioning demands, forcing the whole cross-section to be in compression, which is beneficial for concrete materialization.

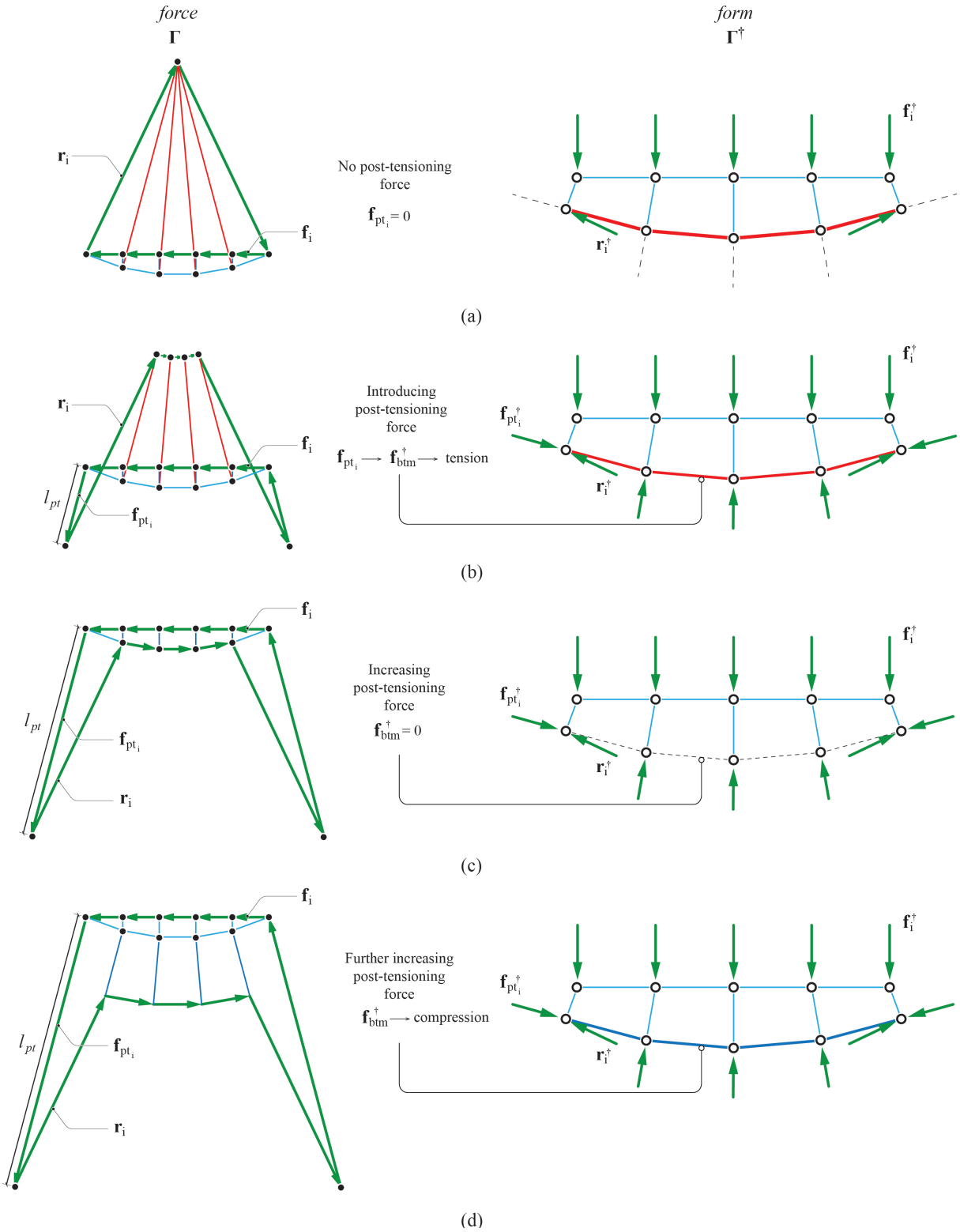


Figure 2. Force and form diagram about applying the post-tensioning force in the incremental phases. The bottom member of the structure turns from tension into compression.

## 3. Materialization

The form-finding method in the previous section demonstrates the manipulation of the integrated post-tensioning force to define the geometric form. Figure 3 presents a systematic process of translating a force

diagram into an optimized structural member, culminating in a design that efficiently utilizes material. This process progresses through several stages, each characterized by specific design operations and fabrication considerations.

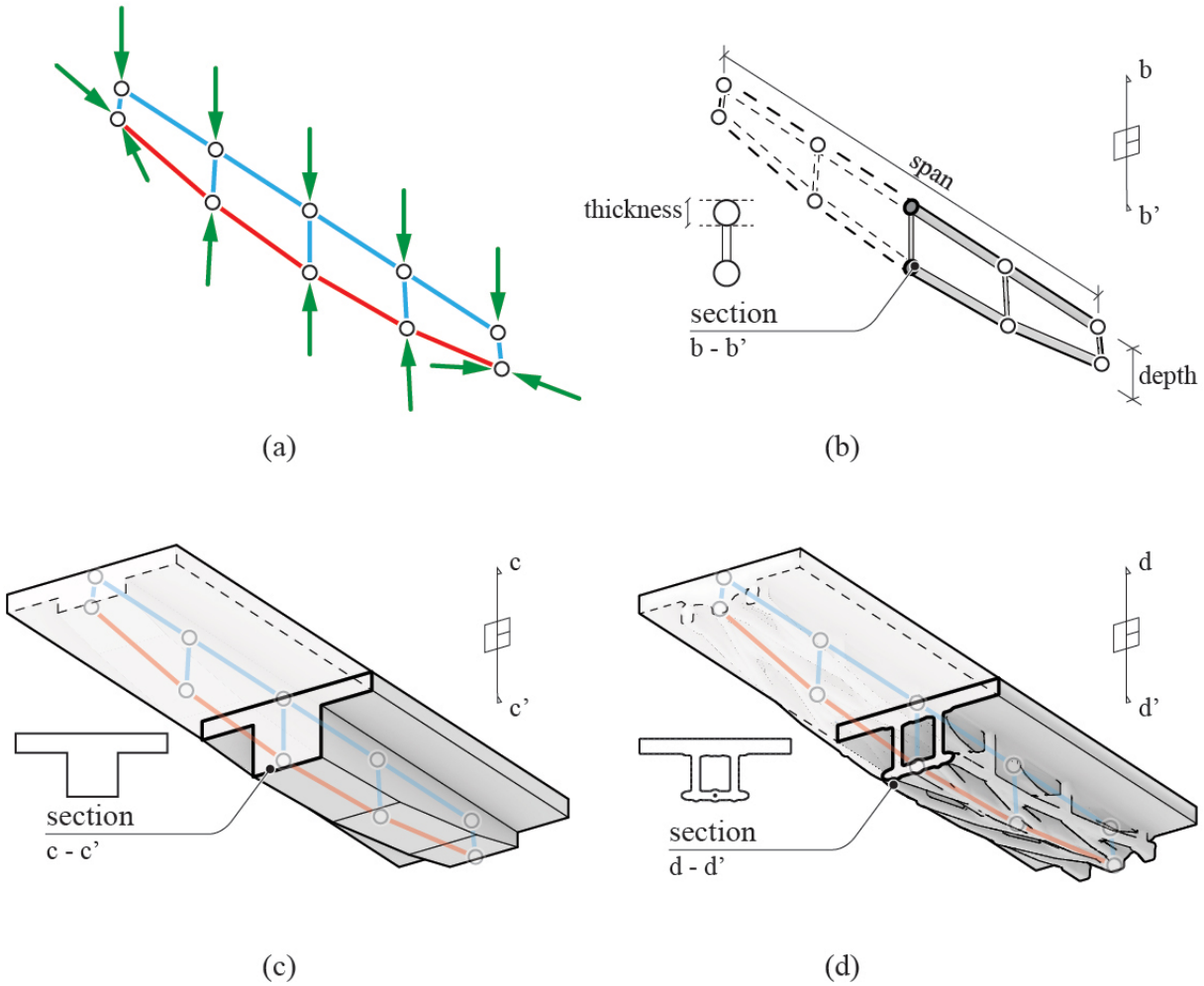


Figure 3. Design exploration of the beam from the initial form to materialized PAS structure. (a) the form diagram defined from the loading and boundary condition; (b) the thickened member represents the relationship between the concrete material of compressive stress and section of the area; (c) the expanded T-shape for the real practice consideration; (d) PAS embedded design for reducing the structure weight through the volume reduction.

Figure 3(a) depicts the resultant form diagram determined in Section 2. This diagram represents a state of equilibrium where the geometry has been determined by the distribution of forces within the structure. Each member's line weight in the form diagram is indicative of the force magnitude it carries, with the blue and red lines suggesting the paths of load transfer, in compression and tension respectively, and the green arrows symbolizing applied loads and resultant reactions.

In Figure 3(b), the linear members from the form diagram undergo a process of thickening. This material augmentation is proportional to the forces exhibited in the corresponding force diagram, ensuring that each member's size is proportional with its load-bearing responsibility. The thickening process ensures that the members' sectional properties align with the performance requirements dictated by the forces they must resist. For designing the concrete structure, if the applied load and the compressive strength of the concrete are known, the estimated cross-sectional area required to resist the compressive force can be calculated as follows:

$$A_{required} \geq \frac{F_{apply}}{f'_c} \tag{1}$$

where $F_{apply}$ is the applied load and $f'_c$ is the compressive strength of the concrete. The location of tension members at the bottom of the form diagram, signified in red in Figure 3(a), inform the placement and general curvature of the post-tensioning steel cable reinforcement.

In Figure 3(c), the abstracted, thickened form is translated into a more defined structural typology, specifically a T-shaped beam. The flange of this beam maintains the thickness of the thickened compression members from the previous step, embodying the load-resistance relationship. The depth and width of the beam's web can be parameterized according to the specifications provided by prevalent concrete design standards and codes to ensure compliance with structural safety and performance criteria.

The culmination of the process is illustrated in Figure 3(d), where the initial volume of the T-beam is transformed by embedding a PAS geometry within it. The application of PAS further optimizes the material distribution within the beam, allowing for a reduction in volume, which in turn reduces the overall weight and material usage of the structure, all while maintaining or even enhancing its structural performance. This design approach facilitates a reduction in concrete volume, aligning with sustainability objectives by lowering the carbon footprint associated with the member's production and utilization.

This procedural evolution from force diagram to an optimized PAS-integrated beam represents a blend of structural design principles with material optimization techniques. It underscores the potential for graphic statics as not merely an analytical tool but as a foundation for innovative structural design. Through this method, the initial form-finding process based on force distribution is materially actualized in a resource-efficient manner, illustrating the seamless transition from theoretical force diagrams to optimized structural elements.

## 4. Structural analysis

In this section, an analytical approach is demonstrated for determining the post-tensioning force $P$ as a numerical method grounded in the principles of statics and strength of materials [13]. A post-tensioning force(s) that causes the whole beam to experience only compression stresses for a given applied distributed load is determined, in particular, tensile stresses are made zero in the cross-section [14]. The post-tensioning force value is related to the graphic statics model in the subsequent section.

Figure 4 presents an approximate sectional analysis of the beam generated in Figure 3(d). This beam is used as an illustrative example for calculating the effects of post-tensioning forces within a structural element that has PAS geometry. The analysis integrates the design geometry with the fundamental principles of structural mechanics and the post-tensioning process, resulting in a comprehensive understanding of the internal stress distribution due to externally applied loads and internally induced forces.

In the mid-span sectional representation shown in Figure 4(a), the key geometric parameters such as flange width ($b_f$), flange thickness ($h_f$), web width ($b_w$), and overall height ($h$) are identified by the designers, establishing the physical dimensions of the beam's cross-section. The centroid of the section is denoted, and the eccentricity ($e$) is defined as the distance between the centroid, the moment of inertia ($I$) is obtained from provided data, and the line of action of the post-tensioning force ($P$), which is located based on the graphic statics model, indicating the non-symmetrical placement of the tendon within the cross-section. The distances from the top and bottom of the section to the centroid are labeled as $C_1$ and $C_2$, respectively.

In Figure 4(b-f), a simplified illustration of the stresses developed in the cross section due to an applied distributed load and the specified post-tensioning force is provided. Figure 4(b) assumes the

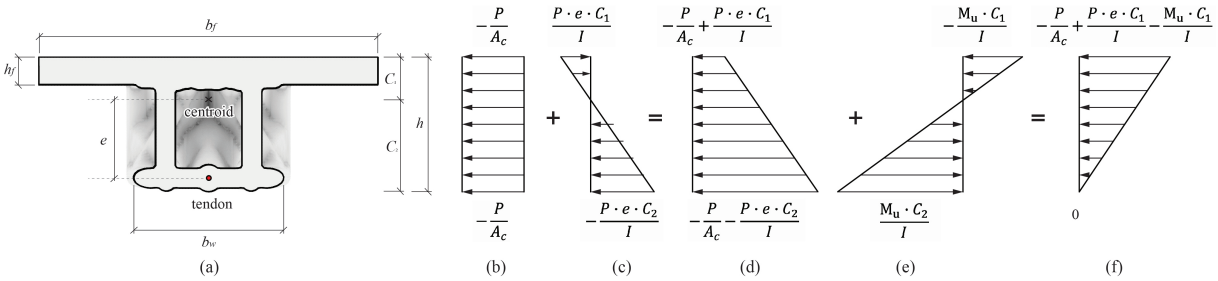


Figure 4. (a) Cross-section at the mid-span; (a) post-tensioning compressive stress; (b) stress caused by post-tensioning eccentricity; (c) the resulting stress caused by (a) and (b); (d) stresses developed by applied load - distributed forces; (e) sum of all the stresses, in which the bottom tensile stress equals to zero.

post-tensioning force, which is constant throughout the cross-section area ($A_c$), developing a constant compression stress $f_C$:

$$f_C = \frac{P}{A_c} \tag{2}$$

The linear stress caused by the post-tensioning force eccentricity at mid-span is illustrated in Figure 4(c), resulting in the cross-section's bottom $f_{btm}$ in the compression and the top $f_{top}$ in tension.

$$f_{top} = \frac{P \cdot e \cdot C_1}{I} \tag{3}$$

$$f_{btm} = -\frac{P \cdot e \cdot C_2}{I} \tag{4}$$

By combining the effects in Figure 4 (b) and (c), the cross-section stress is put into compression as shown in Figure 4(d). Additionally, there are stresses developed by the distributed load on the beam. The bending moment $M_u$ is calculated here using the standard formula for a uniformly loaded simply supported beam:

$$M_u = \frac{w \cdot l^2}{8} \tag{5}$$

where $w$ is the uniformly distributed load and $l$ is the span length.

The intention here is to solve for the post-tension force $P$ that results in the sum of the stress at the bottom of a beam's cross-section equals zero:

$$-\frac{P}{A_c} - \frac{P \cdot e \cdot C_2}{I} + \frac{M_u \cdot C_2}{I} = 0 \tag{6}$$

The post-tensioning force $P$ is solved for by re-arranging the terms to:

$$P = \frac{M_u \cdot C_2 \cdot A_c}{e \cdot C_2 \cdot A_c + I} \tag{7}$$

This condition ensures that the design's cross section does not have any tensile forces, beneficial in fully engaging and utilizing PAS geometries for material efficiency. Overall, the goal is to counterbalance the tensile stresses induced by the applied forces with the compressive forces due to post-tensioning.

## 5. Relating graphic statics to post-tensioning stress development

Linking the geometric form-finding method to the analytical result requires correlating the post-tensioning force represented using graphic statics with the post-tensioning force calculated in Equation (7). An applied, distributed load is considered at the top surface of the beam; here, with respect to graphic statics, this distributed load is represented as multiple point loads applied to a user-defined number of vertices $v_i$ in the force diagram. The magnitude of the applied load is represented by the length of the lines in the force diagram, which is proportional to the specified distributed load applied to the structure.

In order to relate the applied loading condition to graphic statics, the force diagram can be subdivided into an infinite number of vertices to represent the distributed loading. From this assumption, the sum of all the edge lengths of the applied load in the graphic statics model represents the total value of the distributed load. To compare the post-tensioning force $P_{gs}$ determined from graphic statics in Figure 2 with the $P_{solved}$ from Equation (7), the scale of the force diagram must match the actual load values.

Tracing back to the establishment of the form and force diagram that integrates the post-tensioning force, the length of the post-tensioning force $l_{\mathbf{f}_{pt}}$ in Figure 2(c) eliminates tension forces in the bottom members ($\mathbf{f}^{\dagger}_{\text{btm}} = 0$). Hence, the length of $l_{\mathbf{f}_{pt}}$ must be preserved or increased in order to ensure that the bottom tensile stresses of the beam are equal to zero or are in compression. Figure 5 illustrates the relationship starting from the applied load length in the force diagram:

$$l_{\mathbf{f}} = w \cdot l_{span} \tag{8}$$

where $l_{\mathbf{f}}$ is the length of the graphic statics applied loads, $w$ is the applied distributed load along the length of the beam $l_{span}$. Such a relationship between $l_{\mathbf{f}}$ and applied loads at the top of the beam can conservatively lead to the result of the $P_{gs}$. To get the same value based on the relationship and the calculated $P_{solved}$, Figure 6 shows the process of adjusting the length of $l_{\mathbf{f}_{pt}}$ while preserving the predefined loading condition and mid-span depth of the form diagram, which leads to the same section calculation of the $P_{solved}$. The relationship can be described as:

$$\frac{l_{\mathbf{f}}}{l_{\mathbf{f}_{pt}}} = \frac{w \cdot l_{span}}{P_{solved}} \tag{9}$$

Using this relationship, if either the loading and/or the span change, the graphic statics model can immediately indicate the $P_{gs}$, which matches $P_{solved}$.

## 6. Conclusion

This research proposes an implementation between graphic statics and material optimization within the context of structural concrete design, highlighting the potential of integrating anticlastic geometries to

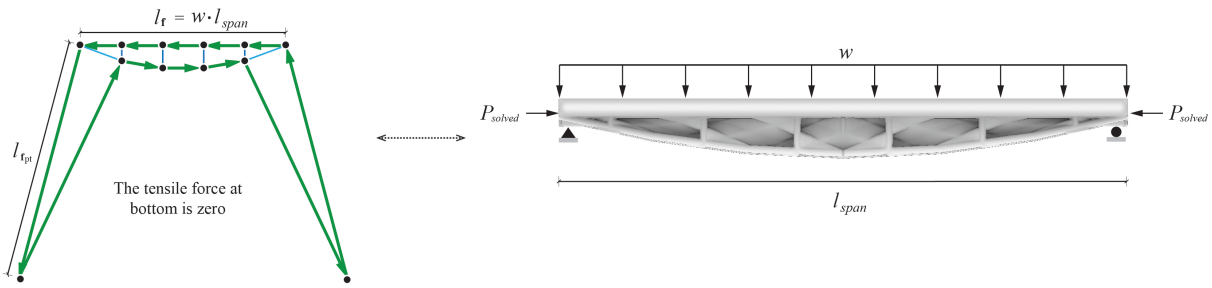


Figure 5. The connection between the graphic statics model and the analytical calculations based on the distributed force $w$ and the span of the beam $l_{span}$.

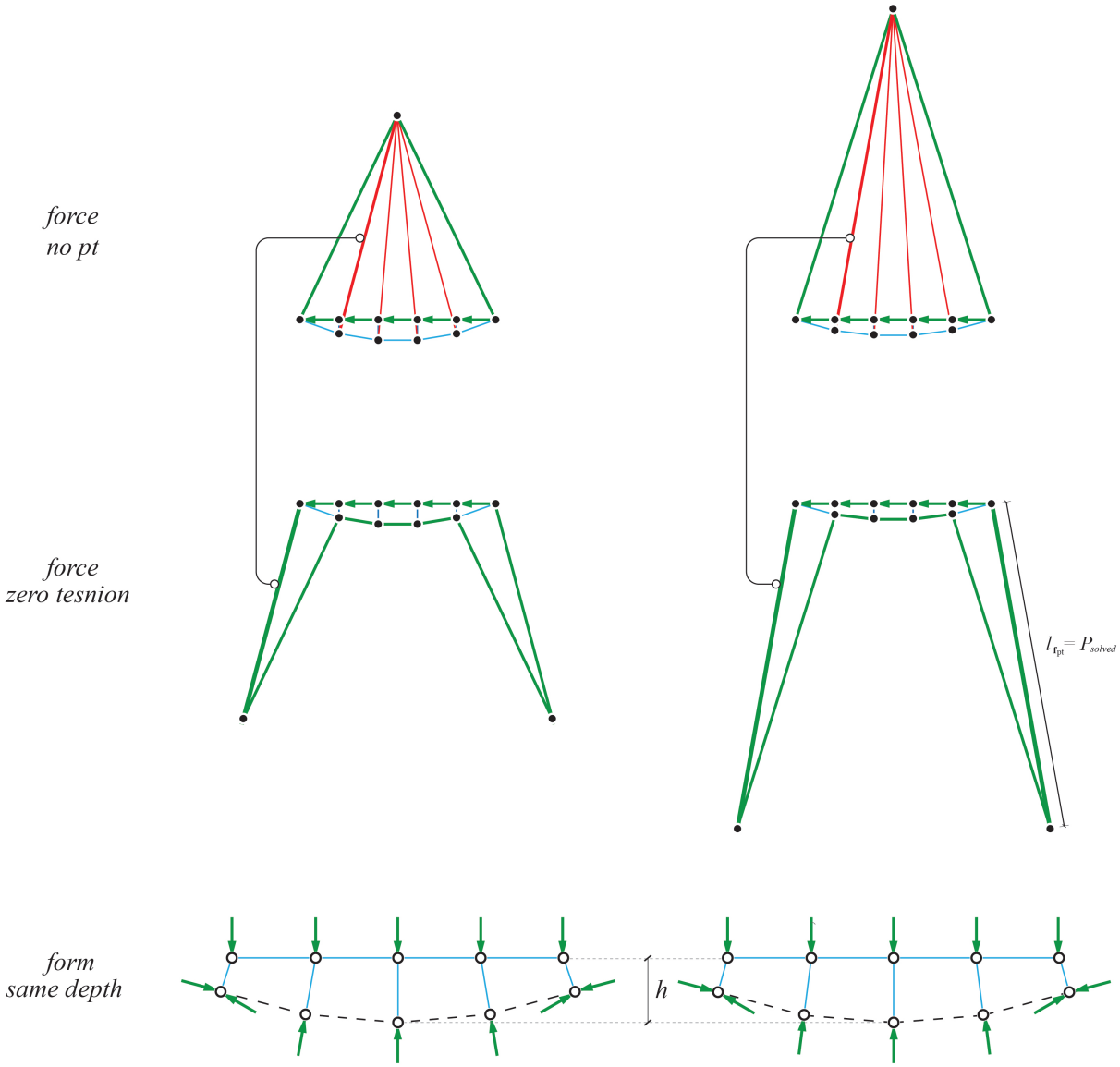


Figure 6. Process of defining the length $l_{\mathbf{f}_{pt}}$ to match the post-tensioning force $P_{solved}$ such that tensile stresses are reduced to zero. Both form diagrams have the same depths $h$ and the force diagrams $l_{\mathbf{f}_{pt}}$ is adjusted accordingly.

enhance sustainability. Through a comprehensive analysis that begins with a form diagram indicative of internal force distributions and advances through stress calculations, the work converges on an optimized structural member design. The calculated post-tensioning force $P$ bridges the graphical and analytical realms, ensuring that the resultant member geometry satisfies both equilibrium and material stress conditions.

Subsequent to analytical validation, the adoption of PAS within the T-beam configuration emerges as a novel strategy to materially economize without compromising structural integrity. This dual approach not only facilitates a significant reduction in concrete volume, addressing environmental sustainability goals, but also exemplifies integration of form and function.

## Acknowledgements

This research is funded by the Advanced Research Projects Agency–Energy (ARPA-E) of the U.S. Department of Energy (DE-AR0001631) and the National Science Foundation CAREER Award (NSF

CAREER-1944691 CMMI) to Dr. Masoud Akbarzadeh.

## References

[1] IEA. (2022) World energy outlook 2022. https://www.iea.org/reports/world-energy-outlook-2022.
[2] J. Lehne and F. Preston, *Making concrete change; innovation in low-carbon cement and concrete*. Chatham House Report, 2018.
[3] J. C. Maxwell, "On Reciprocal Figures and Diagrams of Forces," *Philosophical Magazine Series 4*, vol. 27, no. 182, pp. 250–261, 1864.
[4] M. Akbarzadeh, "3d graphic statics using reciprocal polyhedral diagrams," Ph.D. dissertation, ETH Zurich, Zurich, Switzerland, 2016.
[5] M. Akbari, A. Mirabolghasemi, M. Bolhassani, A. Akbarzadeh, and M. Akbarzadeh, "Strut-based cellular to shellular funicular materials," *Advanced Functional Materials*, p. 2109725, 2022.
[6] Y. Lu, M. Cregan, P. Chhadeh, A. Seyedahmadian, M. Bolhassani, J. Schneider, J. Yost, and M. Akbarzadeh, "All glass, compression-dominant polyhedral bridge prototype: form-finding and fabrication," in *Proceedings of IASS Symposium and Spatial Structures Conference 2020/21, Inspiring the next generation*, Guildford, UK, August 23-27 2021.
[7] M. Akbarzadeh and M. Hablicsek, "Algebraic 3d graphic statics: Constrained areas," *arXiv preprint arXiv:2007.15133*, 2020.
[8] Y. Lu, M. Hablicsek, and M. Akbarzadeh, "Algebraic 3d graphic statics with edge and vertex constraints: A comprehensive approach to extending the solution space for polyhedral form-finding," *Computer-Aided Design*, In peer-review.
[9] X. Y. Jiawei Feng, Jianzhong Fu and Y. He, "Triply periodic minimal surface (tpms) porous structures: from multi-scale design, precise additive manufacturing to multidisciplinary applications," *International Journal of Extreme Manufacturing*, 2022.
[10] M. Bernhard, M. Bolhassani, and M. Akbarzadeh, "Performative Porosity – adaptive infills for concrete parts," in *Proceedings of the IASS Annual Symposium 2020/21*, Surrey, UK, 2021.
[11] M. AKBARI, M. AKBARZADEH, and M. BOLHASSANI, "From polyhedral to anticlastic funicular spatial structures," in *Proceedings of IASS Symposium*, 2019.
[12] H. Chai, Y. Lu, M. Hablicsek, and M. Akbarzadeh, "Generation of a compression-tension combined funicular polyhedral beam structure," in *Proceedings of the IASS Annual Symposium 2023 Integration of Design and Fabrication*, Melbourne, Australia, July 10-14 2023.
[13] P.-T. Institute, *Post-tensioning manual*. Post-Tensioning Institute, 1985.
[14] K. D. Bondy and B. Allred, *Post-Tensioned Concrete: Principles and Practice*. Lulu. com, 2017.